

Small-Molecule Integrated Stress Response Inhibitor Reduces Susceptibility to Postinfarct Atrial Fibrillation in Rats via the Inhibition of Integrated Stress Responses^S

Ting Zhang, Yong Wu, Zhengtao Hu, Wen Xing, Kun LV, Deguo Wang, and Nengwei Hu

Department of Gerontology (T.Z., Y.W., Z.H., W.X., D.W., N.H.) and Key Laboratory of Non-Coding RNA Transformation Research of Anhui Higher Education Institution (W.X., K.L., D.W., N.H.), First Affiliated Hospital of Wannan Medical College (Yijishan Hospital), Wuhu, Anhui, China; Department of Psychology, Wannan Medical College, Wuhu, Anhui, China (T.Z.); and Department of Pharmacology & Therapeutics and Institute of Neuroscience, Trinity College, Dublin, Ireland (N.H.)

Received January 06, 2021; accepted June 23, 2021

ABSTRACT

Phosphorylation of the eukaryotic translation initiation factor 2 α -subunit, which subsequently upregulates activating transcription factor 4 (ATF4), is the core event in the integrated stress response (ISR) pathway. Previous studies indicate phosphorylation of eukaryotic translation initiation factor 2 α -subunit in atrial tissue in response to atrial fibrillation (AF). This study investigated the role of ISR pathway in experimental AF by using a small-molecule ISR inhibitor (ISRIB). Accordingly, rats were subjected to coronary artery occlusion to induce myocardial infarction (MI), or sham operation, and received either trans-ISRIB (2 mg/kg/d, i.p.) or vehicle for seven days. Thereafter, animals were subjected to the AF inducibility test by trans-esophageal rapid burst pacing followed by procurement of left atrium (LA) for assessment of atrial fibrosis, inflammatory indices, autophagy-related proteins, ISR activation, ion channel, and connexin 43 expression. Results showed a significant increase in the AF vulnerability and the activation of ISR in LA as evidenced by enhanced eukaryotic translation initiation factor 2 α -subunit phosphorylation. ISRIB treatment suppressed upregulation of ATF4, fibrosis as indexed by determination of α -smooth muscle actin and collagen levels, inflammatory macrophage infiltration (i.e., CD68 and inducible nitric oxide

synthase/CD68-positive macrophage), and autophagy as determined by expression of light chain 3. Further, ISRIB treatment reversed the expression of relevant ion channel (i.e., the voltage-gated sodium channel **1.5**, L-type voltage-dependent calcium channel 1.2, and voltage-activated A-type potassium ion channel 4.3) and connexin 43 remodeling. Collectively, the results suggest that the ISR is a key pathway in pathogenesis of AF, post-MI, and represents a novel target for treatment of AF.

SIGNIFICANCE STATEMENT

The activation of integrated stress response (ISR) pathway as evidenced by enhanced eukaryotic translation initiation factor 2 α -subunit phosphorylation in left atrium plays a key role in atrial fibrillation (AF). ISR inhibitor (ISRIB) reduces AF occurrence and atrial proarrhythmic substrate. The beneficial action of ISRIB may be mediated by suppressing ISR pathway-related cardiac fibrosis, inflammatory macrophage infiltration, autophagy, and restoring the expression of ion channel and connexin 43. This study suggests a key dysfunctional role for ISR in pathogenesis of AF with implications for novel treatment.

Introduction

Atrial fibrillation (AF) is the most common sustained arrhythmia in clinical practice, and associated with stroke, congestive heart failure, and mortality (Guo et al., 2015; Lippi et al., 2020). With the aging of the population, AF has become a remarkable

public health problem (Krijthe et al., 2013) associated with high costs of medical care of affected individuals (Stewart et al., 2002). Nowadays, available therapies for AF include antiarrhythmic drug, catheter ablation, and surgical ablation, each with limitations like adverse effects, inconsistent efficacy, and high recurrence rates (Heijman et al., 2016). Recent studies identified new pathophysiological mechanisms of AF, including cardiac fibrosis (Nattel, 2017), oxidative stress (Antonopoulos et al., 2019), apoptosis, autophagy (Chen et al., 2011; Wiersma et al., 2017), inflammation (Zhou and Dudley, 2020), atrial ion-channel dysfunction, Ca^{2+} -handling abnormalities, autonomic neural dysregulation, and atrial remodeling (Andrade et al., 2014).

This work was supported by the National Natural Science Foundation of China [Grant 81670301].

We have no conflict of interest to disclose.

<https://dx.doi.org/10.1124/jpet.121.000491>.

^S This article has supplemental material available at jpet.aspetjournals.org.

ABBREVIATIONS: AF, atrial fibrillation; ATF4, activating transcription factor 4; Cav1.2, L-type voltage-dependent calcium channel 1.2; CD68, Cluster of differentiation (CD)68; Cx43, connexin 43; EF, ejection fraction; eIF2 α , eukaryotic translation initiation factor 2 α -subunit, FS; fractional shortening; iNOS, inducible isoform of nitric oxide synthase; ISR, integrated stress response; ISRIB, integrated stress response inhibitor; Kv4.3, voltage-activated A-type potassium ion channel 4.3; LA, left atrium; LAD, left anterior descending; LC3, light chain 3; LVIDs, internal diameter of left ventricular at end-systole; MI, myocardial infarction; Nav1.5, voltage-gated sodium channel **1.5**; p-eIF2 α , phosphorylated eIF2 α ; PR interval, the time from the onset of the P wave to the start of the QRS complex; α -SMA, α smooth muscle actin.

AF mechanism might be associated with the integrated stress response (ISR), which is always activated in chronic and persistent stress (Pakos-Zebrucka et al., 2016; Santos-Ribeiro et al., 2018). The ISR pathway is upregulated in atria of AF animal models indicated by enhanced phosphorylation of eukaryotic translation initiation factor 2 α (eIF2 α) and subsequently upregulation of activating transcription factor 4 (ATF4) (Pakos-Zebrucka et al., 2016). Previous studies have demonstrated eIF2 α phosphorylation and ATF4 upregulation in the atria of experimental and human AF (Meyer-Roxlau et al., 2017; Wiersma et al., 2017; Freundt et al., 2018). ISR is also involved in atrial inflammation during chronic and persistent stress because it triggers artery inflammasome, interleukin-1 β secretion, and atherosclerosis (Onat et al., 2019).

A novel small-molecule ISR inhibitor (ISRIB) suppresses eIF2 α cascade (Zyryanova et al., 2018; Kenner et al., 2019) and provides beneficial effects in neurodegenerative diseases (Sekine et al., 2015; Rabouw et al., 2019), atherosclerosis (Onat et al., 2019), and cancer (Mahameed et al., 2020). Rabouw et al. (2019) has demonstrated that ISRIB can mitigate undesirable outcomes of low-level ISR activation that may manifest neurologic disease but leaves the cytoprotective effects of acute ISR activation intact. Therefore, we hypothesize that ISRIB may inhibit atrial fibrosis, inflammation, autophagy, dysfunction of ion channel, and AF susceptibility, because chronic stress plays important role of in atrial remodeling and AF (Zhang et al., 2014; Wiersma et al., 2017).

Methods

Animals and Drugs. This study used 60 male rats (Sprague-Dawley, weight 200–250 g). All experimental procedures and protocols used in this study were approved by Animal Care and Use Ethics Committee of Yijishan Hospital (20180022) and performed in accordance with Guideline for the Care and Use of Laboratory Animals of the National Institutes of Health's guideline principles. To achieve myocardial infarction (MI), 30 rats underwent left anterior descending (LAD) ligation, and the other 30 performed a sham operation without artery occlusion (Wu et al., 2020). After 24 hours, both MI and sham control animals were randomly divided into subgroups that received trans-ISRIB (Sigma, SML0843, 2mg/kg/d in 0.5 ml saline, i.p.) or vehicle (0.5 ml saline, i.p.) for seven days. The dosage selection of trans-ISRIB was based on our pretest (Supplemental Material) and previous reports with minor modifications (Barragán-Iglesias et al., 2019; Onat et al., 2019). The high dose of ISRIB (5 mg/kg) led to reduced animal activity and body weight loss (Supplemental Fig. 4), whereas low dose of ISRIB (0.25 mg/kg/d) did not inhibit myocardial inflammation (Supplemental Fig. 3, A and B) (Barragán-Iglesias et al., 2019; Onat et al., 2019). Thus, we used 2 mg/kg/d of ISRIB for our studies. Seven days after administration of ISRIB or vehicle, all rats underwent echocardiographic and electrocardiographic studies.

Myocardial Infarction. MI was induced by coronary artery ligation at the site of the LAD as we have previously described (Wang et al., 2011, 2017; Zhu et al., 2015; Wu et al., 2020). The success of the MI protocol was judged by the ST-segment elevation on ECG (RM6240, Chengdu, China) and pallor transition in heart immediately after ligation. Rats in sham groups underwent the same procedures without LAD occlusion (Wu et al., 2020).

Ultrasound Cardiogram. Seven days after MI, cardiac function was assessed blindly by a skilled echocardiologist (Zhu et al., 2015) using an HP SONOS 5500 (Philips Medical System, Ultrasound Inc.), which was equipped with a 21 MHz ultrasound transducer. Parasternal long-axis and short-axis views were acquired to measure the internal diameters of the left ventricles at end-diastole and end-systole (LVIDs). The ejection fraction (EF) and the fractional shortening (FS) were calculated (Wang et al., 2011).

ECG and AF Inducibility. The ECG trace was continuously recorded by a biologic signal recording and analysis system (RM6240, Chengdu, China) which filtered out the signals below 10 Hz and above 100 Hz. The basic ECG was recorded consciously for 10 minutes for calculating ECG parameters such as P wave, QRS complex, PR interval (the time from the onset of the P wave to the start of the QRS complex), and QT intervals (the time from the beginning of the QRS complex to the end of the T wave) (Wang et al., 2011; Wu et al., 2020). The AF inducibility was performed by the transesophageal burst rapid pacing with a stimulating amplitude of 2-fold atrial capture threshold. Four consecutive bursts of rapid electrical stimulation for 30s (20, 30, 40, and 50 Hz) were applied to induce AF with 3-minute pause (Cheng et al., 2019). AF was defined as an abnormal ECG showing rapid and fragmented P wave with absolute irregular RR intervals (the time elapsed between two successive R-waves of the QRS signal on the electrocardiogram) for at least 2 seconds (Cheng et al., 2019). The inducibility of AF was determined by the percentage of animals with induced AF. The duration of the longest episodes of AF was taken as inducible AF duration (Hohl et al., 2017).

Masson Staining. Six left atrial (LA) tissue samples were dissected from every group and fixed in 4% paraformaldehyde, embedded in paraffin, and cut into sections (5 μ m thick). Sections of LA were stained by Masson's staining to detect collagen as previously reported (Wang et al., 2016). The level of cardiac fibrosis was determined by the percentage of the fibrosis area to the total area (% cardiac fibrosis) using the ImageJ software (Media Cybernetics, Inc.) (Wu et al., 2020).

Immunohistochemistry and Immunofluorescence Labeling. Paraffin-embedded tissue sections of LA were processed and incubated with different primary antibodies (Supplemental Table 1) at 4°C overnight (Wang et al., 2011). For immunohistochemistry, six sections from every group were stained with the Envision system (Dako) and counterstained with hematoxylin. For immunofluorescence, secondary antibodies conjugated with fluorescein (Fluorescein isothiocyanate/CY3) were incubated for 1 hour at room temperature. Then, 4,6-diamino-2-phenylindole was used to counterstain nuclei for further evaluation. The negative control staining was performed using the same protocol without adding any primary antibody. Images were recorded using a microscope (Nikon Eclipse C1, Tokyo, Japan) and quantified using the ImageJ software through calculating as the percentage of positively stained area to total area at high magnification ($\times 400$). For quantification of CD68⁺ macrophages, the number of cells was counted in high magnification fields.

Western Blot. Protein expression was assayed using Western blot as described previously (Wang et al., 2019). In brief,

TABLE 1
Echocardiographic data of experimental groups

	Sham + Vehicle	Sham + ISIRIB	MI + Vehicle	MI + ISIRIB
	<i>n</i> = 11	<i>n</i> = 12	<i>n</i> = 11	<i>n</i> = 12
LVIDd (cm)	0.615 ± 0.037	0.609 ± 0.044	0.716 ± 0.053	0.648 ± 0.052
LVIDs (cm)	0.290 ± 0.025	0.298 ± 0.028	0.478 ± 0.043*	0.336 ± 0.032 [#]
LVPWd (cm)	0.199 ± 0.011	0.181 ± 0.012	0.185 ± 0.014	0.192 ± 0.015
EDV (ml)	0.523 ± 0.108	0.561 ± 0.118	0.848 ± 0.156	0.658 ± 0.122
ESV (ml)	0.435 ± 0.098	0.457 ± 0.108	0.581 ± 0.132	0.524 ± 0.144
EF (%)	87.138 ± 3.821	85.805 ± 4.11	48.659 ± 2.38**	67.326 ± 3.477 ^{**##}
FS (%)	53.443 ± 2.867	52.672 ± 2.958	25.675 ± 2.308**	38.647 ± 2.903 ^{*#}

LVIDd, left ventricular internal diameter at end-diastole; LVPWd, left ventricular posterior wall thickness at end-diastole; EDV, end-diastolic volume; ESV, end-systolic volume; LVPWs, left ventricular posterior wall thickness at end-systole; All data are shown as mean ± S.E.M. Multiple groups were assessed using one-way ANOVA followed by the post hoc Newman-Keuls multiple comparison test.

P* < 0.05, *P* < 0.01 versus Sham group; [#]*P* < 0.05, ^{##}*P* < 0.01 versus MI group.

six LA tissues from each group were processed, and protein concentrations measured by the bicinchoninic acid assay. Equal amounts of proteins (50 µg) were separated using 5% SDS-PAGE and transferred onto a polyvinylidene fluoride membrane. The membrane was then blocked with 5% nonfat dry milk in blocking buffer (10 mM Tris-HCl, 150 mM NaCl, and 0.2% Tween-20, pH 7.6) for 2 hours at 37°C and incubated with primary antibodies (seen in Supplemental Table 1) at certain dilutions at 4°C overnight. The antibody binding was detected using a horseradish peroxidase-conjugated secondary antibody (1:2000; Sigma) and visualized using an enhanced chemiluminescence kit for quantification for blots image (a Quantity-One software, Bio-Rad).

Statistical Analysis. Values were expressed as means ± S.E.M. Significant differences between means were determined using the one-way ANOVA coupled with the Bonferroni post hoc test for multiple comparisons. The Mann-Whitney *U* test was used to test the difference of AF duration between the two MI groups. The χ^2 test was used to compare the inducibility of AF. A value of *P* < 0.05 was considered significant difference.

Results

ISIRIB Improves Cardiac Function in Post-MI Rats. Within the first 24 hours, 2 rats and 4 rats died in sham and

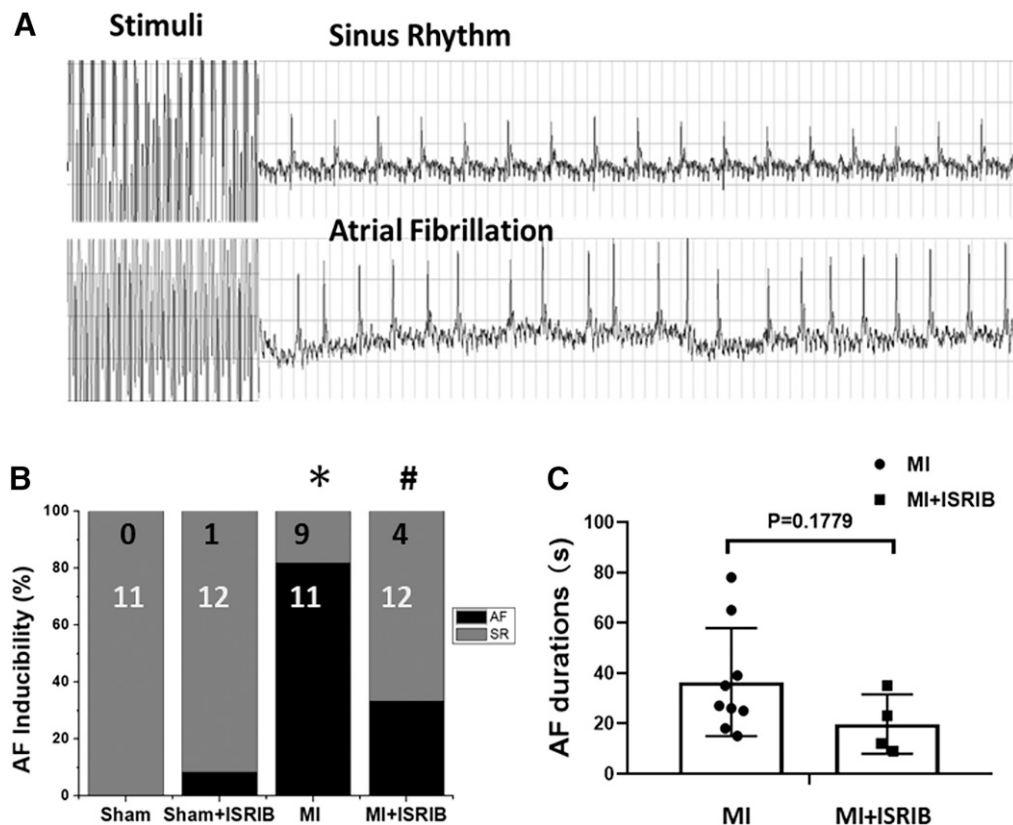


Fig. 1. Effects of ISIRIB on AF inducibility and duration post-MI. (A) Representative images of ECG (lead II) with sinus rhythm and AF by a burst of rapid pacing. (B) Inducibility of AF. (C) Durations of induced AF. Data are shown as means ± S.E.M. The χ^2 test was used to compare the inducibility of atrial fibrillation. The Mann-Whitney *U* test was used to test the difference of AF duration between the two MI groups. **P* < 0.05 versus sham group; [#]*P* < 0.05 versus MI group.

TABLE 2
Characterization of the surface ECG

	Sham + Vehicle	Sham + ISRIB	MI + Vehicle	MI + ISRIB
	<i>n</i> = 11	<i>n</i> = 12	<i>n</i> = 11	<i>n</i> = 12
Heart rate (bpm)	425.3 ± 6.9	418.6 ± 6.7	445.3 ± 7.8	438.6 ± 6.5
P (ms)	21.62 ± 0.67	23.45 ± 0.85	35.44 ± 0.78**	26.02 ± 0.92***
PR (ms)	46.45 ± 1.23	48.38 ± 1.16	53.77 ± 1.82**	46.73 ± 1.32##
QRS (ms)	22.65 ± 0.43	23.65 ± 0.61	38.73 ± 0.68**	26.69 ± 0.71***
QT (ms)	51.98 ± 1.89	54.42 ± 1.79	64.55 ± 1.18**	53.61 ± 1.57##

All data are shown as mean ± S.E.M. Significant differences between means were determined using one-way ANOVA with the Bonferroni post hoc test for multiple comparisons. bpm, beats-per-minute; ms, microsecond.
P* < 0.05, *P* < 0.01 versus Sham group; #*P* < 0.05, ##*P* < 0.01 versus MI group.

MI group, respectively (13.3% versus 26.7%, *P* = 0.3894). From the second day, remaining rats received ISRIB or vehicle injection. On the second and third days, 2 rats died in MI group and one rat died in each of the other three groups (Supplemental Fig. 1). No significant differences in animal survival rate were noted between sham and MI groups with or without ISRIB intervention (*P* = 0.8571). On the seventh day, two rats in the sham group and one rat in the sham + ISRIB group died while under anesthesia and, thus, did not complete ultrasound cardiogram and ECG assessment (Supplemental Fig. 1). To assess whether ISRIB administration affects cardiac function post-MI, we investigated the echocardiographic parameters after ISRIB treatment in post-MI rats (Table 1). As shown in Table 1, rats in the MI group exhibited significantly reduced EF (%) and FS (%), expanded cardiac systolic volume, and LVIDs compared with sham group. ISRIB treatment significantly ameliorated the decline of EF, FS, and ventricular enlargement in MI rats, but the treatment did not affect the aforementioned parameters in sham-operated animals.

ISRIB Inhibits AF Inducibility in Post-MI Rats. To determine whether ISRIB may be beneficial in AF, we tested the AF inducibility and ECG parameters in post-MI rats. Figure 1A shows that atrial burst rapid pacing could induce AF. Compared with the sham group, the MI group exhibited significant vulnerability to AF (81.82% versus 0%, *P* < 0.05). ISRIB significantly reduced the AF inducibility in MI rats (33.3% versus 81.82%, *P* < 0.05) (Fig. 1B). The longest AF duration was not different between the two MI groups (Fig. 1C). We also observed increases in P wave duration, QRS wave complexes, PR interval, and QT interval compared with the sham group (*P* < 0.01). ISRIB significantly reduced these changes in MI rats (*P* < 0.01, Table 2).

ISRIB Prevents Atrial Fibrosis in the LA in Post-MI Rats. Figure 2A shows representative illustrations for atrial fibrosis. ISRIB treatment significantly reduced fibrotic areas of the LA in MI rats but not in normal rats (Fig. 2D). As shown in Fig. 2B, the expression levels of the α-smooth muscle actin (α-SMA, a marker for the proliferation of myofibroblasts) in

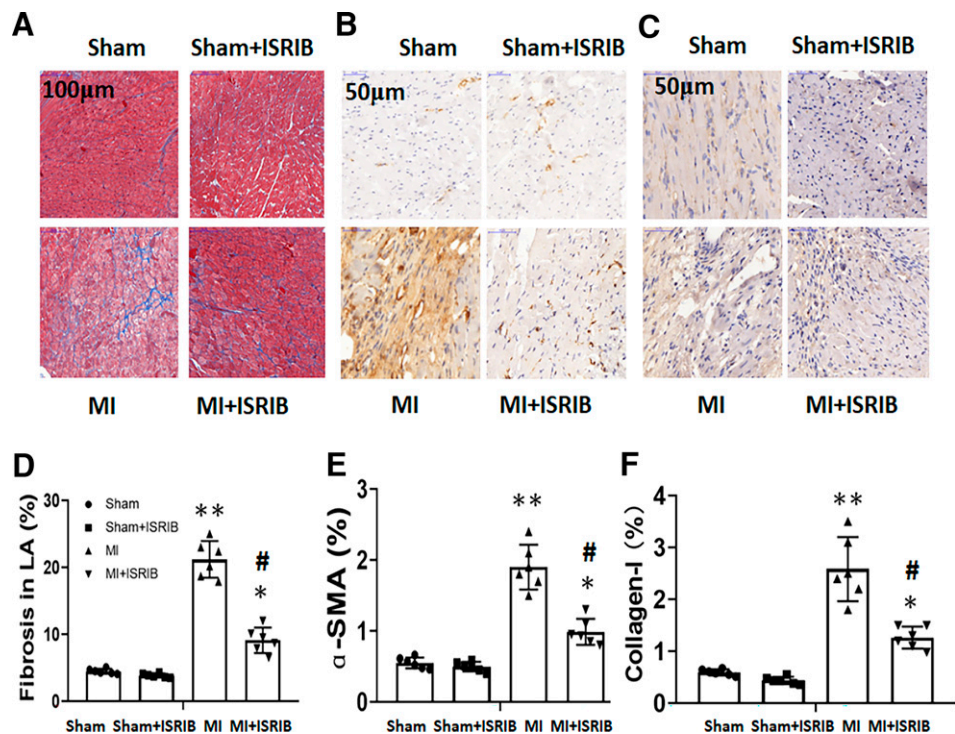


Fig. 2. Effects of ISRIB on the interstitial fibrosis of the LA post-MI. (A–C) Representative images of left atrial tissues at 7 days post-MI subjected to the Masson trichrome staining, α-SMA, or collagen I immunohistochemistry. (D–F) Quantitative analysis of fibrosis, α-SMA, and type I collagen volume fraction. Data are shown as means ± S.E.M. Differences between means were determined by one-way ANOVA with the Bonferroni post hoc test for multiple comparisons. **P* < 0.05, ***P* < 0.01 versus sham group; #*P* < 0.05, ##*P* < 0.01 versus MI group.

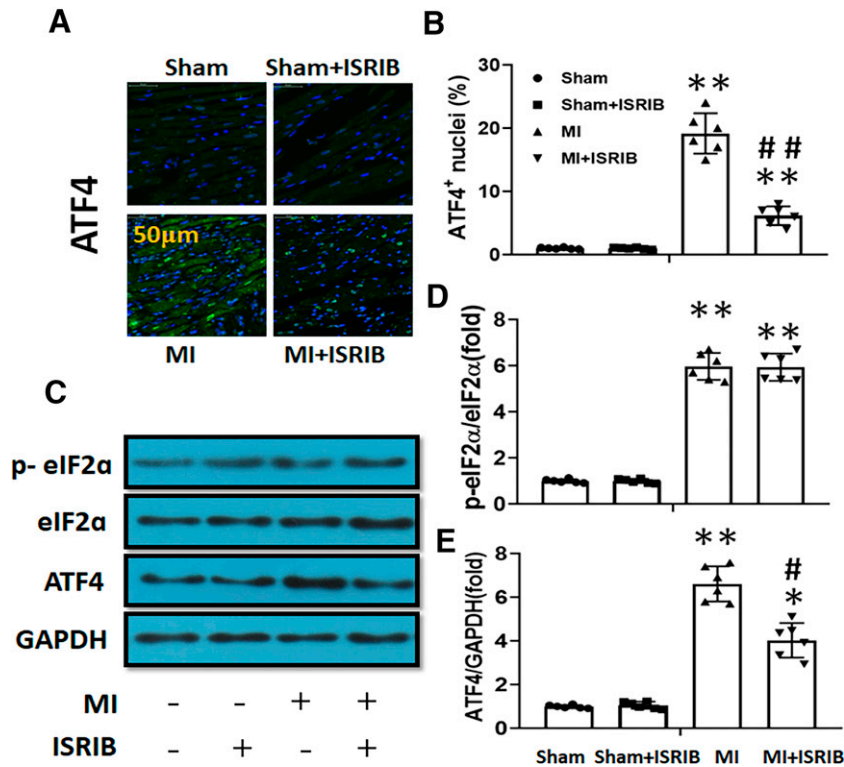


Fig. 3. Effects of ISRIB on the atrial expression of eIF2 α and ATF4 post-MI. (A) Representative fluorescent immunostaining images of ATF4 in the left atria at seven days after MI (Scale bar = 50 μ m). (B) Quantitative assessment of ATF4-positive nuclei in the left atria. (C) Representative Western blot images of total eIF2 α , p-eIF2 α , and ATF4 in atria. (D) Quantitative analysis of the expression of phosphorylated eIF2 α relative to total eIF2 α . (E) Quantitative analysis of the expression of ATF4 relative to GAPDH. Data are shown as means \pm S.E.M. Significant differences between means were determined by one-way ANOVA with the Bonferroni post hoc test for multiple comparisons. * P < 0.05, ** P < 0.01 versus sham group; # P < 0.05, ## P < 0.01 versus MI group.

rats were significantly higher than those in normal rats. ISRIB significantly ameliorated the α -SMA expression in LA from the MI group, but not from the normal group (Fig. 2E). As shown in Fig. 3C, a remarkable deposition of collagen I in the LA of the MI group was observed compared with that of the sham group. ISRIB treatment significantly reduced collagen I productions in MI rats but not in normal rats (Fig. 2F). These results indicated that ISR had a role in atrial fibrosis by promoting myofibroblast transition and collagen deposition after MI.

ISRIB Restores ATF4 Expression without Affecting Phosphorylated eIF2 α in the LA in Post-MI Rats. ISR activation leads to global reduction in protein synthesis but preferentially enhances translation of some mRNAs such as ATF4. Using fluorescent immunostaining, we found that the level of ATF4 remarkably increased in LA from MI group compared with sham group (Fig. 3, A and B). ISRIB treatment significantly reversed ATF4 level in post-MI rats (Fig. 3, A and B). Western blot further confirmed that ISRIB treatment significantly inhibited the ATF4 protein expression in the LA from MI rats but not from normal rats (Fig. 3, C and E). The key regulation step in the ISR is the phosphorylation of eIF2 α . We found that ISRIB treatment did not alter the expression levels of eIF2 α and phosphorylated eIF2 α (p-eIF2 α) in both sham and MI rats (Fig. 3, C and D). These results indicate that ISRIB restores ATF4 protein expression in the nuclei of myocytes from LA through suppressing the downstream of the eIF2 α pathway.

ISRIB Regulates Atrial Macrophage Infiltration in Post-MI Rats. Previous studies have reported inflammatory response and macrophage infiltration in atrial tissue including

M1 (iNOS⁺/CD68⁺) and M2 subtypes (CD163⁺/CD68⁺) (Sun et al., 2016; Liu et al., 2019). As shown in Fig. 4, A and C, a remarkable increase of total CD68⁺ macrophages was observed in LA from MI rats, which could be reduced by ISRIB treatment. Moreover, the distributions of iNOS-positive and CD163-positive immunofluorescence signals are not limited to macrophages and increase significantly in atrial tissue from MI rats (Fig. 4, A and B). ISRIB treatment reduced iNOS⁺/CD68⁺ cells (Fig. 4D) without changing CD163⁺/CD68⁺ cells (Fig. 4E). These results indicate that ISR may play an important role in macrophages infiltration into atrial tissue from post-MI rats.

ISRIB Modulates the Expression of Autophagy-Related Protein in the LA in Post-MI Rats. We also determined the expression of autophagy markers, LC3, which is activated and incorporated into autophagosomes (Wiersma et al., 2017; Yuan et al., 2018). Using fluorescent immunostaining, we found a significant increase in the expression of the autophagy marker LC3 in LA in MI rats, which was completely reversed by ISRIB (Fig. 5, A and C). Western blot analysis also confirmed an increase of LC3-II and LC3-II/LC3-I ratio in LA, and ISRIB treatment significantly reduced the upregulation of LC3 in MI rats (Fig. 5, B and D). These results suggest a biological contribution of ISR to endoplasmic reticulum stress and autophagy.

ISRIB Stabilizes the Connexin 43 Expression in the LA in Post-MI Rats. To determine whether the reduction in ISR activation affects the Cx43 expression and distribution in atria, we tested the Cx43 level using fluorescent

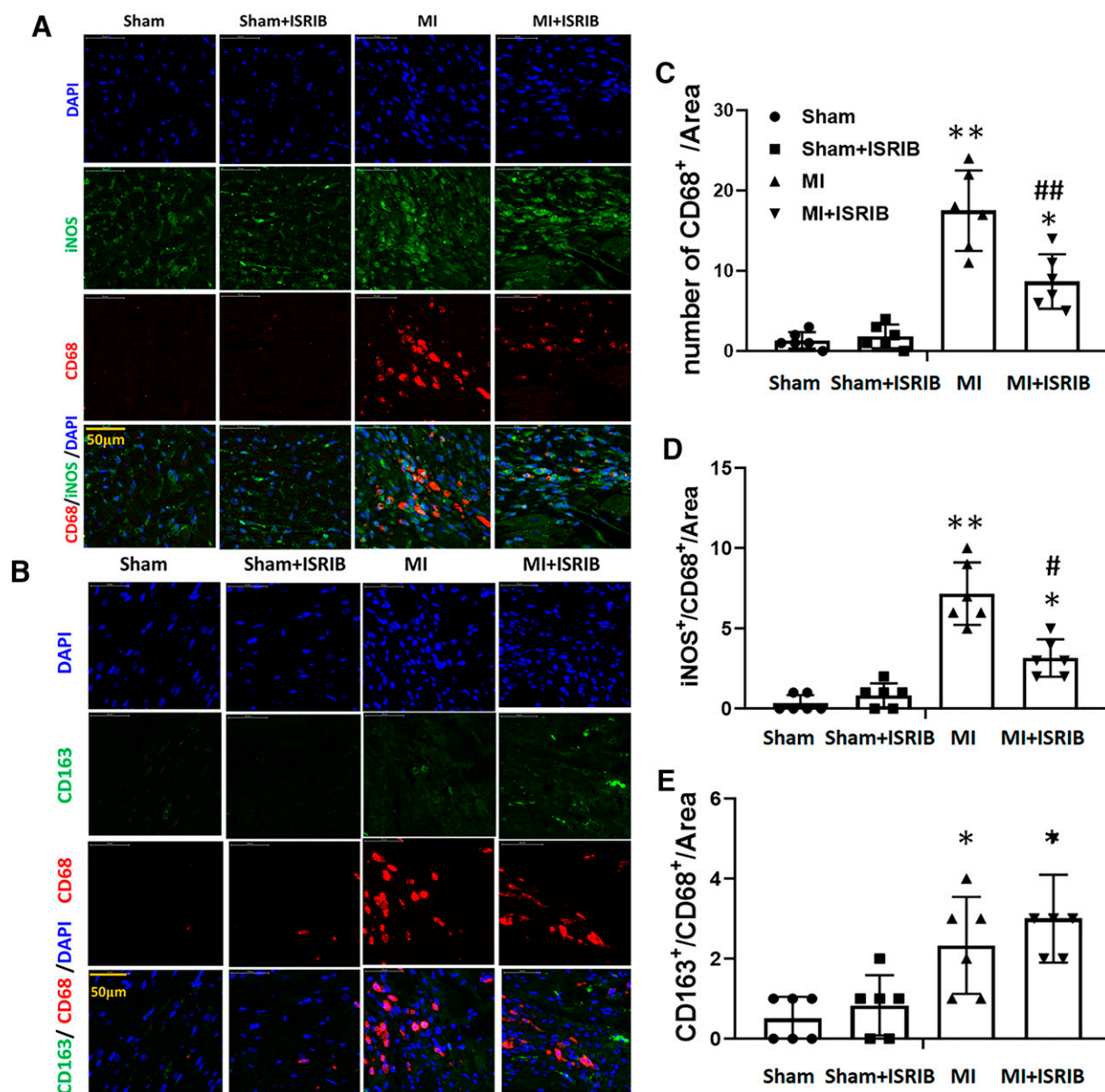


Fig. 4. Effects of ISRIB on the atrial inflammation post-MI. (A and B) Representative fluorescent immunostaining images of inflammatory cell infiltration in the left atria at seven days after MI (Scale bar = 50 μ m). (C–E) Quantitative assessment of CD68, iNOS, or CD163 and CD68-positive (CD68⁺, iNOS⁺/CD68⁺, and CD163⁺/CD68⁺) area of cells. Data are shown as means \pm S.E.M. Significant differences between means were determined by one-way ANOVA with the Bonferroni post hoc test for multiple comparisons. * P < 0.05, ** P < 0.01 versus sham group; # P < 0.05, ### P < 0.01 versus MI group.

immunostaining. The Cx43 was distributed in the intercalated disk (end of myocardial cell) in the sham-operated group but redistributed to the lateral cell membrane in the MI group (Supplemental Fig. 2, A and B). As shown in Fig. 6A, Cx43 immunostaining was markedly reduced in LA in MI rats. Accordingly, the relative value of the Cx43-positive area decreased significantly in the MI group, which was reversed by ISRIB treatment (Fig. 6B). These results suggest that the ISR activation may be associated with the gap junction remodeling.

ISRIB Keeps Ion Channel Expression in the LA in Post-MI Rat. The abnormal ion channel is closely related to the action potentials of atrial myocytes, which facilitate atrial re-entry via the atrial heterogeneous conduction and focal trigger activity (Nattel et al., 2007). The protein expression of

some ion channel-related proteins [such as Nav1.5, L-type calcium channel α 1c (Cav1.2), and Kv4.3], which are involved in AF, were assessed to learn the role of ISR in the generation of AF (Nattel et al., 2007). We found significant reduction in protein expression for Nav1.5 (Fig. 7, A and B), Cav1.2 (Fig. 7, A and C), and Kv4.3 (Fig. 7, A and C) in LA in MI rats (Fig. 7). Moreover, ISRIB treatment significantly restored the protein expression levels of all three ion channels (Fig. 7). These results support the notion that ISR results in the downregulation of the protein expression of the above ion channels in LA.

Discussion

This study demonstrates that ISR activation in the LA is associated with post-MI AF. We have also observed that MI

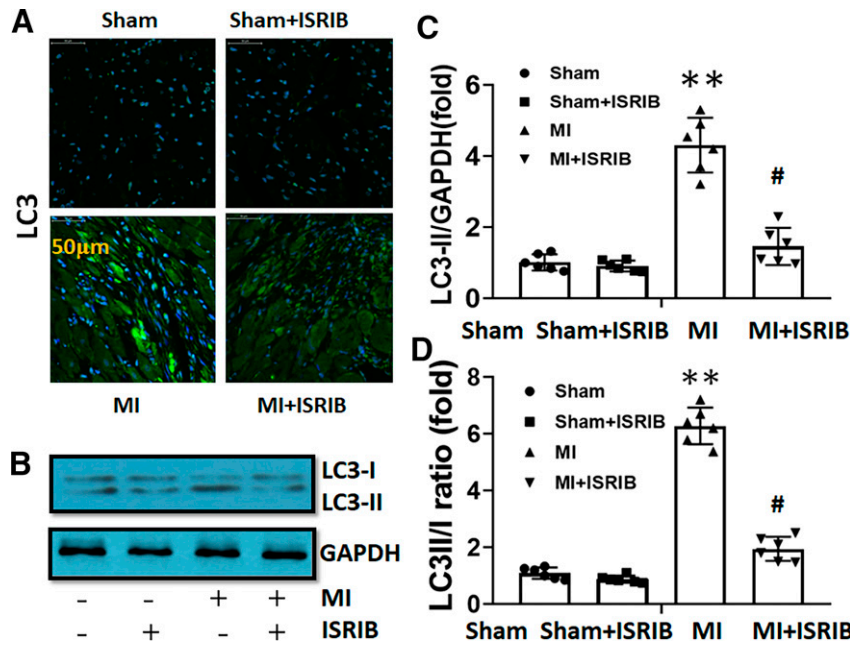


Fig. 5. Effects of ISRIB on the atrial expression of autophagy-related protein post-MI. (A) Representative fluorescent immunostaining images of autophagy-related protein LC3 (green) in the left atria at seven days after MI (Scale bar = 50 μ m). (B) Representative Western blot images of the autophagy-related protein LC3 in the left atria. (C and D) Quantitative analysis of the expression of LC3-II relative to GAPDH and the ratio of LC3-II to LC3-I. Data are shown as means \pm S.E.M. Significant differences between means were determined by one-way ANOVA with the Bonferroni post hoc test for multiple comparisons. * P < 0.05, ** P < 0.01 versus sham group; # P < 0.05, ## P < 0.01 versus MI group.

promoted atrial fibrosis, inflammation, autophagy, and down-regulated protein expression level of Cx43 and ion-channel subunits including Nav1.5, Cav1.2, and Kv4.3. A small-molecule ISR inhibitor called ISRIB (trans-ISRIB) ameliorated left ventricular dysfunction and AF inducibility accompanied with reduced atrial inflammation, fibrosis, and autophagy, as well as reversal of protein expression of ion channels and Cx43 in the LA post-MI.

We observed that ISRIB restored aberrant high ATF4 protein expression in the LA from MI rats without changing total eIF2 α and p-eIF2 α . As the core event in the ISR pathway, the phosphorylation of eIF2 α leads to the upregulation of ATF4

and the prohibition of global protein synthesis (Pakos-Zebrucka et al., 2016). ISRIB enhances long-term memory and ameliorates neurodegenerative diseases (Sekine et al., 2015; Sidrauski et al., 2015; Chou et al., 2017; Tsai et al., 2018). It mitigates low-level ISR activation and keeps acute ISR activation intact, which is helpful for neurologic diseases (Rabouw et al., 2019). Thus, ISRIB may protect against chronic ISR-related diseases such as atherosclerosis (Onat et al., 2019) and type 2 diabetes mellitus (Pandey et al., 2019). Recent studies indicate the involvement of endoplasmic reticulum stress, which appeared as upregulation of eIF2 α and ATF4, in atria of experimental and human AF (Wiersma et al., 2017; Freundt et al., 2018). Therefore, ISRIB may inhibit AF by suppressing ISR in atria. Indeed, the present study showed that ISRIB significantly reduced the AF inducibility to rapid atrial stimulation. We deduce that ISR may be involved in the atrial proarrhythmic substrates of AF in post-MI rats.

The atrial fibrosis is associated with low-conduction velocity and long activation time (Krul et al., 2015). Suppression of atrial fibrosis prevents AF through upstream therapy, including renin-angiotensin-aldosterone system, inflammatory mediators, and other signaling targets (Li et al., 2001; Nattel et al., 2020). Under stress conditions, the transforming growth factor β 1 promotes fibroblasts to proliferate and differentiate into profibrotic collagen-secreting myofibroblasts, leading to atrial collagen deposition, extracellular matrix remodeling, and fibrosis (Nattel et al., 2020). In the present study, we observed that the ISRIB reduced more than 50% of the fibrotic areas and inhibited the collagen type I deposition and α -SMA expression in the LA from MI rats, thereby suggesting that ISR is involved in atrial fibrosis.

The atrial inflammation mediates electrical and structural remodeling and modulates calcium homeostasis and gap

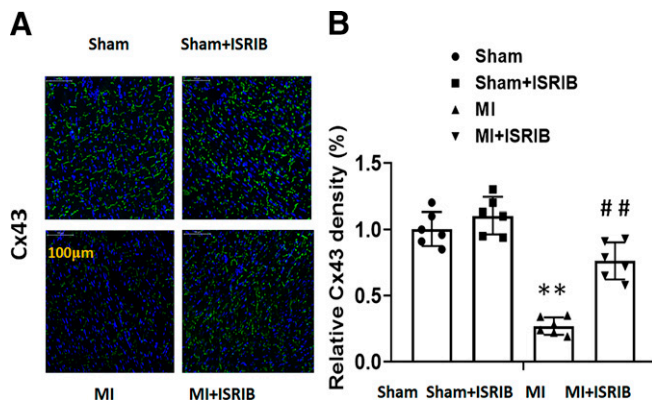


Fig. 6. Effects of ISRIB on atrial expression of Cx43 post-MI. (A) Representative fluorescent immunostaining images of Cx43 (green) in the left atria at 7 days after MI (Scale bar = 100 μ m). (B) Quantitative assessment of Cx43 expression in the left atria. Data are shown as means \pm S.E.M. Significant differences between means were determined by one-way ANOVA with Bonferroni post hoc test for multiple comparisons. * P < 0.05, ** P < 0.01 versus sham group; # P < 0.05, ## P < 0.01 versus MI group.

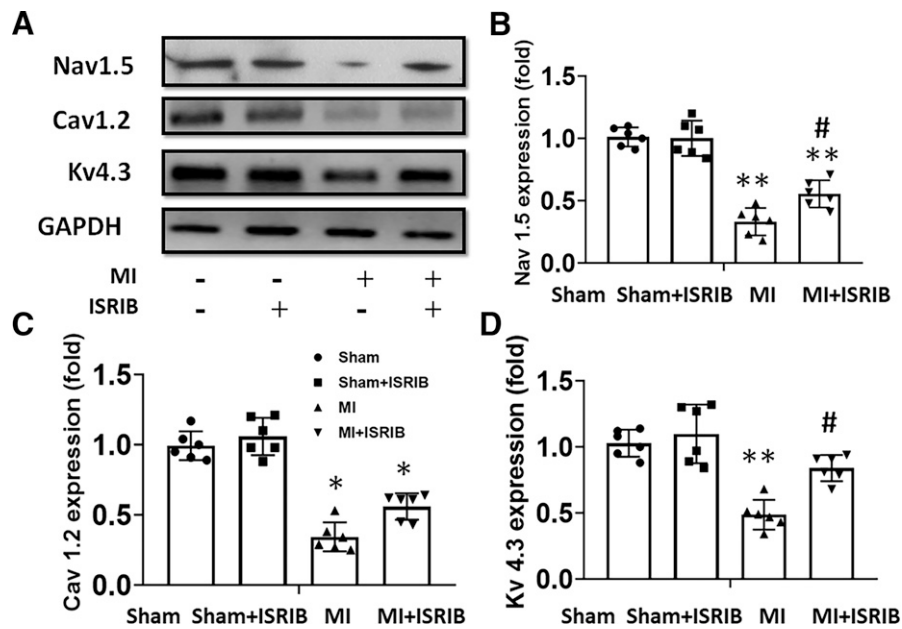


Fig. 7. Effects of ISRIB on atrial expression of the ion channel protein post-MI. (A) Representative Western blot images of ion channel protein in the left atria at seven days after MI. (B–D) Quantitative analysis of the expression levels of Nav1.5, Cav1.2, and Kv4.3 relative to GAPDH. Data are shown as means \pm S.E.M. Significant differences between means were determined by one-way ANOVA with Bonferroni post hoc test for multiple comparisons. * $P < 0.05$, ** $P < 0.01$ versus sham group; # $P < 0.05$, ## $P < 0.01$ versus MI group.

junction (Hu et al., 2015; Packer, 2020). Patients with AF have an increased immune cell infiltration in the atria, such as CD45⁺ lymphocytes, CD68⁺ macrophages (Chen et al., 2008), CD163⁺ macrophages (Watson et al., 2020), and proinflammatory cytokines (Zhou and Dudley, 2020). The suppression of atrial inflammation has antiarrhythmic effects against AF in the early phase of MI (Deftereos et al., 2012; Lakin et al., 2019; Liu et al., 2019; Zhou and Dudley, 2020). In this study, ISRIB reduces total CD68⁺ macrophage infiltration in LA, suggesting involvement of ISR in atrial inflammation. We also observed that some infiltrated CD68⁺ macrophages in LA from MI rats were iNOS-positive, but CD163-negative. ISRIB treatment reduced the level of iNOS but not CD163 in atria. CD163-positive macrophages, which have been known as a marker of M2 subtype (Liu et al., 2019), also have potential profibrotic role in atrium from AF (Watson et al., 2020). Thus, the ISR plays an important role in regulating atrial proinflammatory response. Further study is needed to clarify the detailed mechanism of ISR in atrial inflammation and the occurrence of AF.

Previous studies have showed that the autophagy-related protein LC3 increased in the left atrium of human chronic AF (Shingu et al., 2020) and AF animals (Wiersma et al., 2017; Yuan et al., 2018). Our results showed that MI promoted LC3 expression in LA, which was partly reversed by ISRIB treatment. Autophagy may be an important mechanism of AF (Kroemer et al., 2010), because previous studies have confirmed that autophagy could induce atrial electrical remodeling, including L-type Ca²⁺-current reduction and selective degradation of Cav1.2 (Wiersma et al., 2017; Yuan et al., 2018). Autophagy also leads to eIF2 α phosphorylation and ATF4 upregulation in experimental and human AF (Wiersma et al., 2017). Thus, ISR activation might be associated with autophagy and play an important role of AF post-MI.

Several ion channels and gap junctions are involved in electrical remodeling promoting AF (Nattel et al., 2007, 2020) and facilitate atrial re-entry and focal trigger activity (Nattel et al., 2007). Reduction of the Nav1.5 expression contributes to AF by delaying conduction and promoting re-entry (Martin et al., 2019; McCauley et al., 2020). The protein and gene expression levels of voltage-dependent K⁺ channel 4.3 (Kv4.3) are down-regulated in atria from AF patients and models (Brundel et al., 2001a,b; Bosch et al., 2003). The protein and gene expression of Cav1.2 decreased in LA in models of atrial tachycardia (Nakatani et al., 2013; Martins et al., 2014; Chong et al., 2015). In the present study, we found that ISRIB ameliorates the reduction in the protein expression levels of Nav1.5, Cav1.2, and Kv4.2 in LA from post-MI. We also found that ISRIB improves the Cx43 expression and distribution. Cx43 is a major component of gap junction between myocytes, and its abnormality may cause atrial spatial heterogeneity of conduction (Nattel et al., 2007). In a rat model of spontaneous hypertension, the AF vulnerability is associated with slow conduction velocity and low Cx43 expression, phosphorylation, and redistribution (Parikh et al., 2013). Thus, our results suggest that ISRIB may attenuate the atrial electrical remodeling by preventing the downregulation of functional transmembrane proteins, including ion channel and Cx43 in LA.

As key mechanisms of initial and maintenance of AF, ion channels and gap junction may be altered by ischemia through atrial fibrosis (Nattel, 2017), inflammation (Zhou and Dudley, 2020), and autophagy in LA (Wiersma et al., 2017; Packer, 2020). In the present study, ISRIB inhibited atrial fibrosis, inflammation, and autophagy in LA. Therefore, ISR pathway might contribute to the proarrhythmic mechanism of AF. Overall, ISRIB blocks the ATF4 protein expression without affecting p-eIF2 α in LA post-MI, which results in the restoration of normal functional protein synthesis (including ion

channels and gap junction) by suppressing the downstream of the eIF2 α pathway.

This study has several limitations. First, we did not determine spontaneous AF in nonanesthesia rats due to lack of relevant physiologic monitoring system for small animals. Second, we did not evaluate the electrophysiological functions of ion channel (Na⁺, K⁺, and Ca²⁺) from atrial myocytes, although we have determined the protein expression of Nav1.5, Cav1.2, and Kv4.2. Third, other signaling pathways relevant to ISR may also play roles in AF. Fourth, further studies are needed to establish the long-term therapeutic effects of ISIRIB on AF in the context of assessment of its potential toxic effects.

Conclusions

Despite the existence of several limitations, this study has revealed that the trans-ISIRIB could suppress ISR in ischemia atria, which are at risk for AF. The possible mechanisms may be related to cardiac fibrosis, inflammatory cell infiltration, autophagy-related protein LC3 expression, and the remodeling of ion channel and Cx43. Considering the limitations of current therapies for AF, this study suggests that the ISR is a key pathway in pathogenesis of AF and represents a novel target for treatment of AF.

Acknowledgments

We thank Professor He Yang for valuable assistance in writing this manuscript.

Authorship Contributions

Participated in research design: Lv, Wang.

Conducted experiments: Zhang, Wu, Hu.

Contributed new reagents or analytic tools: Zhang.

Performed data analysis: Xing, Wang.

Wrote or contributed to the writing of the manuscript: Hu, Wang.

References

- Andrade J, Khairy P, Dobrev D, and Nattel S (2014) The clinical profile and pathophysiology of atrial fibrillation: relationships among clinical features, epidemiology, and mechanisms. *Circ Res* **114**:1453–1468.
- Antonopoulos AS, Goliopoulou A, Oikonomou E, Tsalamandris S, Papamikroulis GA, Lazaros G, Tsiamis E, Latsios G, Brili S, Papaioannou S, et al. (2019) Redox state in atrial fibrillation pathogenesis and relevant therapeutic approaches. *Curr Med Chem* **26**:765–779.
- Barragán-Iglesias P, Kuhn J, Vidal-Cantú GC, Salinas-Abarca AB, Granados-Soto V, Dussor GO, Campbell ZT, and Price TJ (2019) Activation of the integrated stress response in nociceptors drives methylglyoxal-induced pain. *Pain* **160**:160–171.
- Bosch RF, Scherer CR, Rüb N, Wöhrl S, Steinmeyer K, Haase H, Busch AE, Seipel L, and Kühlkamp V (2003) Molecular mechanisms of early electrical remodeling: transcriptional downregulation of ion channel subunits reduces I(Ca,L) and I(to) in rapid atrial pacing in rabbits. *J Am Coll Cardiol* **41**:858–869.
- Brundel BJ, Van Gelder IC, Henning RH, Tieleman RG, Tuinenburg AE, Wietes M, Grandjean JG, Van Gilst WH, and Crijns HJ (2001a) Ion channel remodeling is related to intraoperative atrial effective refractory periods in patients with paroxysmal and persistent atrial fibrillation. *Circulation* **103**:684–690.
- Brundel BJ, Van Gelder IC, Henning RH, Tuinenburg AE, Wietes M, Grandjean JG, Wilde AA, Van Gilst WH, and Crijns HJ (2001b) Alterations in potassium channel gene expression in atria of patients with persistent and paroxysmal atrial fibrillation: differential regulation of protein and mRNA levels for K⁺ channels. *J Am Coll Cardiol* **37**:926–932.
- Chen MC, Chang JP, Liu WH, Yang CH, Chen YL, Tsai TH, Wang YH, and Pan KL (2008) Increased inflammatory cell infiltration in the atrial myocardium of patients with atrial fibrillation. *Am J Cardiol* **102**:861–865.
- Chen MC, Chang JP, Wang YH, Liu WH, Ho WC, and Chang HW (2011) Autophagy as a mechanism for myolysis of cardiomyocytes in mitral regurgitation. *Eur J Clin Invest* **41**:299–307.
- Cheng C, Liu H, Tan C, Tong D, Zhao Y, Liu X, Si W, Wang L, Liang L, Li J, et al. (2019) Mutation in *NPPA* causes atrial fibrillation by activating inflammation and cardiac fibrosis in a knock-in rat model. *FASEB J* **33**:8878–8891.
- Chong E, Chang SL, Hsiao YW, Singhal R, Liu SH, Leha T, Lin WY, Hsu CP, Chen YC, Chen YJ, et al. (2015) Resveratrol, a red wine antioxidant, reduces atrial fibrillation susceptibility in the failing heart by PI3K/AKT/eNOS signaling pathway activation. *Heart Rhythm* **12**:1046–1056.
- Chou A, Krukowski K, Jopson T, Zhu PJ, Costa-Mattioli M, Walter P, and Rosi S (2017) Inhibition of the integrated stress response reverses cognitive deficits after traumatic brain injury. *Proc Natl Acad Sci USA* **114**:E6420–E6426.
- Deftereos S, Giannopoulos G, Kossyvakis C, Efremidis M, Panagopoulou V, Kaoukis A, Raisakis K, Bouras G, Angelidis C, Theodorakis A, et al. (2012) Colchicine for prevention of early atrial fibrillation recurrence after pulmonary vein isolation: a randomized controlled study. *J Am Coll Cardiol* **60**:1790–1796.
- Freundt JK, Frommeyer G, Wötzel F, Hüge A, Hoffmeier A, Martens S, Eckardt L, and Lange PS (2018) The transcription factor ATF4 promotes expression of cell stress genes and cardiomyocyte death in a cellular model of atrial fibrillation. *BioMed Res Int* **2018**:3694362.
- Guo Y, Tian Y, Wang H, Si Q, Wang Y, and Lip GYH (2015) Prevalence, incidence, and lifetime risk of atrial fibrillation in China: new insights into the global burden of atrial fibrillation. *Chest* **147**:109–119.
- Heijman J, Algalarrondo V, Voigt N, Melka J, Wehrens XH, Dobrev D, and Nattel S (2016) The value of basic research insights into atrial fibrillation mechanisms as a guide to therapeutic innovation: a critical analysis. *Cardiovasc Res* **109**:467–479.
- Hohl M, Lau DH, Müller A, Elliott AD, Linz B, Mahajan R, Hendriks JML, Böhm M, Schotten U, Sanders P, et al. (2017) Concomitant obesity and metabolic syndrome add to the atrial arrhythmogenic phenotype in male hypertensive rats. *J Am Heart Assoc* **6**:6.
- Hu YF, Chen YJ, Lin YJ, and Chen SA (2015) Inflammation and the pathogenesis of atrial fibrillation. *Nat Rev Cardiol* **12**:230–243.
- Kenner LR, Anand AA, Nguyen HC, Myasnikov AG, Klose CJ, McGeever LA, Tsai JC, Miller-Vedam LE, Walter P, and Frost A (2019) eIF2B-catalyzed nucleotide exchange and phosphoregulation by the integrated stress response. *Science* **364**:491–495.
- Krijthe BP, Kunst A, Benjamin EJ, Lip GY, Franco OH, Hofman A, Witteman JC, Stricker BH, and Heeringa J (2013) Projections on the number of individuals with atrial fibrillation in the European Union, from 2000 to 2060. *Eur Heart J* **34**:2746–2751.
- Kroemer G, Mariño G, and Levine B (2010) Autophagy and the integrated stress response. *Mol Cell* **40**:280–293.
- Krul SP, Berger WR, Smit NW, van Amersfoort SC, Driessen AH, van Boven WJ, Fiolet JW, van Ginneken AC, van der Wal AC, de Bakker JM, et al. (2015) Atrial fibrosis and conduction slowing in the left atrial appendage of patients undergoing thoracoscopic surgical pulmonary vein isolation for atrial fibrillation. *Circ Arrhythm Electrophysiol* **8**:288–295.
- Lakin R, Polidovitch N, Yang S, Guzman C, Gao X, Wauchop M, Burns J, Izaddoust-dar F, and Backx PH (2019) Inhibition of soluble TNF α prevents adverse atrial remodeling and atrial arrhythmia susceptibility induced in mice by endurance exercise. *J Mol Cell Cardiol* **129**:165–173.
- Li D, Shinagawa K, Pang L, Leung TK, Cardin S, Wang Z, and Nattel S (2001) Effects of angiotensin-converting enzyme inhibition on the development of the atrial fibrillation substrate in dogs with ventricular tachypacing-induced congestive heart failure. *Circulation* **104**:2608–2614.
- Lippi G, Sanchis-Gomar F, and Cervellin G (2020) Global epidemiology of atrial fibrillation: An increasing epidemic and public health challenge. *Int J Stroke* **16**:217–221.
- Liu M, Li W, Wang H, Yin L, Ye B, Tang Y, and Huang C (2019) CTRP9 ameliorates atrial inflammation, fibrosis, and vulnerability to atrial fibrillation in post-myocardial infarction rats. *J Am Heart Assoc* **8**:e013133.
- Mahameed M, Boukeileh S, Obiedat A, Darawshi O, Dipta P, Rimón A, McLennan G, Fassler R, Reichmann D, Karni R, et al. (2020) Pharmacological induction of selective endoplasmic reticulum retention as a strategy for cancer therapy. *Nat Commun* **11**:1304.
- Martin B, Gabris B, Barakat AF, Henry BL, Giannini M, Reddy RP, Wang X, Romero G, and Salama G (2019) Relaxin reverses maladaptive remodeling of the aged heart through Wnt-signaling. *Sci Rep* **9**:18545.
- Martins RP, Kaur K, Hwang E, Ramirez RJ, Willis BC, Filgueiras-Rama D, Ennis SR, Takemoto Y, Ponce-Balbuena D, Zarzoso M, et al. (2014) Dominant frequency increase rate predicts transition from paroxysmal to long-term persistent atrial fibrillation. *Circulation* **129**:1472–1482.
- McCauley MD, Hong L, Sridhar A, Menon A, Perike S, Zhang M, da Silva IB, Yan J, Bonini MG, Ai X, et al. (2020) Ion channel and structural remodeling in obesity-mediated atrial fibrillation. *Circ Arrhythm Electrophysiol* **13**:e008296.
- Meyer-Roxlau S, Lämmle S, Opitz A, Künzel S, Joos JP, Neef S, Sekeres K, Sossalla S, Schöndube F, Alexiou K, et al. (2017) Differential regulation of protein phosphatase 1 (PP1) isoforms in human heart failure and atrial fibrillation. *Basic Res Cardiol* **112**:43.
- Nakatani Y, Nishida K, Sakabe M, Kataoka N, Sakamoto T, Yamaguchi Y, Iwamoto J, Mizumaki K, Fujiki A, and Inoue H (2013) Tranilast prevents atrial remodeling and development of atrial fibrillation in a canine model of atrial tachycardia and left ventricular dysfunction. *J Am Coll Cardiol* **61**:582–588.
- Nattel S (2017) Molecular and cellular mechanisms of atrial fibrosis in atrial fibrillation. *JACC Clin Electrophysiol* **3**:425–435.
- Nattel S, Heijman J, Zhou L, and Dobrev D (2020) Molecular basis of atrial fibrillation pathophysiology and therapy: A translational perspective. *Circ Res* **127**:51–72.
- Nattel S, Maguy A, Le Bouter S, and Yeh YH (2007) Arrhythmogenic ion-channel remodeling in the heart: heart failure, myocardial infarction, and atrial fibrillation. *Physiol Rev* **87**:425–456.
- Onat UI, Yildirim AD, Tufanli Ö, Çimen I, Kocatürk B, Veli Z, Hamid SM, Shimada K, Chen S, Sin J, et al. (2019) Intercepting the lipid-induced integrated stress response reduces atherosclerosis. *J Am Coll Cardiol* **73**:1149–1169.
- Packer M (2020) Characterization, pathogenesis, and clinical implications of inflammation-related atrial myopathy as an important cause of atrial fibrillation. *J Am Heart Assoc* **9**:e015343.
- Pakos-Zebrucka K, Koryga I, Mnich K, Lujic M, Samali A, and Gorman AM (2016) The integrated stress response. *EMBO Rep* **17**:1374–1395.

- Pandey VK, Mathur A, Khan MF, and Kakkar P (2019) Activation of PERK-eIF2 α -ATF4 pathway contributes to diabetic hepatotoxicity: attenuation of ER stress by morin. *Cell Signal* **59**:41–52.
- Parikh A, Patel D, McTiernan CF, Xiang W, Haney J, Yang L, Lin B, Kaplan AD, Bett GC, Rasmusson RL, et al. (2013) Relaxin suppresses atrial fibrillation by reversing fibrosis and myocyte hypertrophy and increasing conduction velocity and sodium current in spontaneously hypertensive rat hearts. *Circ Res* **113**:313–321.
- Rabouw HH, Langeris MA, Anand AA, Visser LJ, de Groot RJ, Walter P, and van Kuppeveld FJM (2019) Small molecule ISRIB suppresses the integrated stress response within a defined window of activation. *Proc Natl Acad Sci USA* **116**:2097–2102.
- Santos-Ribeiro D, Godinas L, Pilette C, and Perros F (2018) The integrated stress response system in cardiovascular disease. *Drug Discov Today* **23**:920–929.
- Sekine Y, Zyryanova A, Crespiello-Casado A, Fischer PM, Harding HP, and Ron D (2015) Stress responses. Mutations in a translation initiation factor identify the target of a memory-enhancing compound. *Science* **348**:1027–1030.
- Shingu Y, Takada S, Yokota T, Shirakawa R, Yamada A, Ooka T, Katoh H, Kubota S, and Matsui Y (2020) Correlation between increased atrial expression of genes related to fatty acid metabolism and autophagy in patients with chronic atrial fibrillation. *PLoS One* **15**:e0224713.
- Sidrauski C, McGeachy AM, Ingolia NT, and Walter P (2015) The small molecule ISRIB reverses the effects of eIF2 α phosphorylation on translation and stress granule assembly. *eLife* **4**:4.
- Stewart S, Hart CL, Hole DJ, and McMurray JJ (2002) A population-based study of the long-term risks associated with atrial fibrillation: 20-year follow-up of the Renfrew/Paisley study. *Am J Med* **113**:359–364.
- Sun Z, Zhou D, Xie X, Wang S, Wang Z, Zhao W, Xu H, and Zheng L (2016) Cross-talk between macrophages and atrial myocytes in atrial fibrillation. *Basic Res Cardiol* **111**:63.
- Tsai JC, Miller-Vedam LE, Anand AA, Jaishankar P, Nguyen HC, Renslo AR, Frost A, and Walter P (2018) Structure of the nucleotide exchange factor eIF2B reveals mechanism of memory-enhancing molecule. *Science* **359**:359.
- Wang D, Wu Y, Chen Y, Wang A, Lv K, Kong X, He Y and Hu N (2019) Focal selective chemo-ablation of spinal cardiac afferent nerve by resiniferatoxin protects the heart from pressure overload-induced hypertrophy. *Biomedicine & pharmacotherapy = Biomedecine & pharmacotherapie* **109**:377–385.
- Wang D, Zhang F, Shen W, Chen M, Yang B, Zhang Y, and Cao K (2011) Mesenchymal stem cell injection ameliorates the inducibility of ventricular arrhythmias after myocardial infarction in rats. *Int J Cardiol* **152**:314–320.
- Wang D, Zhu H, Yang Q and Sun Y (2016) Effects of relaxin on cardiac fibrosis, apoptosis, and tachyarrhythmia in rats with myocardial infarction. *Biomedicine & pharmacotherapy = Biomedecine & pharmacotherapie* **84**:348–355.
- Wang HJ, Rozanski GJ, and Zucker IH (2017) Cardiac sympathetic afferent reflex control of cardiac function in normal and chronic heart failure states. *J Physiol* **595**:2519–2534.
- Watson CJ, Glezeva N, Horgan S, Gallagher J, Phelan D, McDonald K, Tolan M, Baugh J, Collier P, and Ledwidge M (2020) Atrial tissue pro-fibrotic M2 macrophage marker CD163+, gene expression of procollagen and B-type natriuretic peptide. *J Am Heart Assoc* **9**:e013416.
- Wiersma M, Meijering RAM, Qi XY, Zhang D, Liu T, Hoogstra-Berends F, Sibon OCM, Henning RH, Nattel S, and Brundel BJJM (2017) Endoplasmic reticulum stress is associated with autophagy and cardiomyocyte remodeling in experimental and human atrial fibrillation. *J Am Heart Assoc* **6**:6.
- Wu Y, Hu Z, Wang D, Lv K, and Hu N (2020) Resiniferatoxin reduces ventricular arrhythmias in heart failure via selectively blunting cardiac sympathetic afferent projection into spinal cord in rats. *Eur J Pharmacol* **867**:172836.
- Yuan Y, Zhao J, Gong Y, Wang D, Wang X, Yun F, Liu Z, Zhang S, Li W, Zhao X, et al. (2018) Autophagy exacerbates electrical remodeling in atrial fibrillation by ubiquitin-dependent degradation of L-type calcium channel. *Cell Death Dis* **9**:873.
- Zhang D, Wu CT, Qi X, Meijering RA, Hoogstra-Berends F, Tadevosyan A, Cubukcuoglu Deniz G, Durdu S, Akar AR, Sibon OC, et al. (2014) Activation of histone deacetylase-6 induces contractile dysfunction through derailment of α -tubulin proteostasis in experimental and human atrial fibrillation. *Circulation* **129**:346–358.
- Zhou X and Dudley Jr SC (2020) Evidence for inflammation as a driver of atrial fibrillation. *Front Cardiovasc Med* **7**:62.
- Zhu H, Sun X, Wang D, Hu N, and Zhang Y (2015) Doxycycline ameliorates aggregation of collagen and atrial natriuretic peptide in murine post-infarction heart. *Eur J Pharmacol* **754**:66–72.
- Zyryanova AF, Weis F, Faille A, Alard AA, Crespiello-Casado A, Sekine Y, Harding HP, Allen F, Parts L, Fromont C, et al. (2018) Binding of ISRIB reveals a regulatory site in the nucleotide exchange factor eIF2B. *Science* **359**:1533–1536.

Address correspondence to: Deguo Wang, 92nd Zheshan Western Rd., Wuhu, Anhui 241001, P.R. China. E-mail: wangdeguo@medmail.com.cn
